Using Fe and Mg in olivine as an indicator of asteroidal hydrothermal alteration.

Anne Sweet
Macalester College
St. Paul MN 55105

Lysa Chizmadia
University of Hawaii
Honolulu, HI 96822

Abstract

Amoeboid Olivine Aggregates (AOAs) found in CO3 meteorites are sensitive indicators of parent body alteration. As water encounters these objects on the parent body asteroid, the Mg-rich olivine, forsterite (Mg_2SiO_4), is replaced with Fe-rich olivine, creating fayalite (Fe_2SiO_4). The calculation of the Fe/Mg ratio of the, along with a visual examination of the ferroan veins and diffusive halos in these features, allows for a classification of the petrologic subtype (3.0-3.8) of the meteorite. By using a scanning electron microscope (SEM) for meteorite mapping, feature identification, and element mapping, as well as an electron microprobe (EMP) for accurate elemental abundance calculation, we were able to accomplish this classification. In this work we present the subtype classification of six new meteorites along with the analysis of two previously studied meteorites as standards.

Introduction

Chondritic meteorites act as time capsules preserved from the formation of the solar system, retaining information about the hydrothermal processes present during that time. These chondrites never experienced melting, as evidenced by the presence of FeNi alloys and nebular objects (*e.g.* chondrules and Calcium-Aluminum Inclusions (CAIs)) throughout the meteorites. Chondrites have a bulk composition that is very similar to that of the sun, reinforcing their primitive natures. Radiocarbon dating using the long-lived radioisotopes (*e.g.* Pb-Pb, U-Th, Sm-Nd, Rb-Sr) can provide us with early information about the solar system. For example, the dating of CAIs show that these objects were formed 4.56 Ga and are the oldest solids to have formed in our solar system.

Although these meteorites are not severely metamorphosed, they have undergone some alteration due to the presence of water and heat. ^{53}Cr-^{53}Mn and ^{129}I ^{129}Xe dating of secondary carbonates show that aqueous alteration occurred 1-4 Ma after the formation of CAIs.[1] Understanding this alteration sequence allows for a better understanding of how the heat and water were distributed on the parent body asteroid. Currently there are two main models detailing the alteration patterns, the onion skin model, and the plum pudding model (Figure 1).

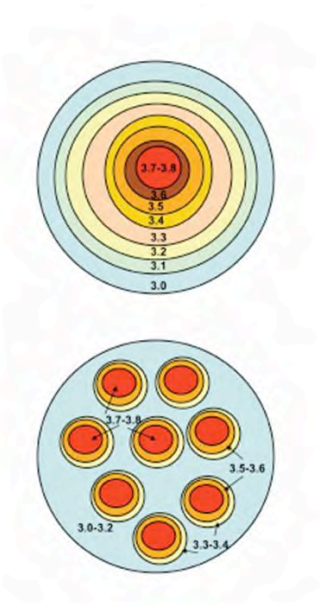

Fig. 1: Schematic showing the two preferred models for asteroidal alteration patterns. The first, the onion skin model shows all the alteration occurring in a layered process, with the most alteration occurring in the center, whereas the second, the plum-pudding model, shows several different alteration centers scattered throughout the parent body.

Although it is not currently known which model accurately represents the alteration on the parent body, the study and classification of the meteorites into subtypes will help to create a statistical basis on which conclusions can be made.

Background

Meteorites are divided into several different categories based on composition. The primary distinction is made on the basis of the presence of chondrules. Chondrules are mm-sized igneous spherules surrounded by matrix. Matrix is the 1-10 μm fine-grained material surrounding the larger objects in a meteorite (Figure 2).

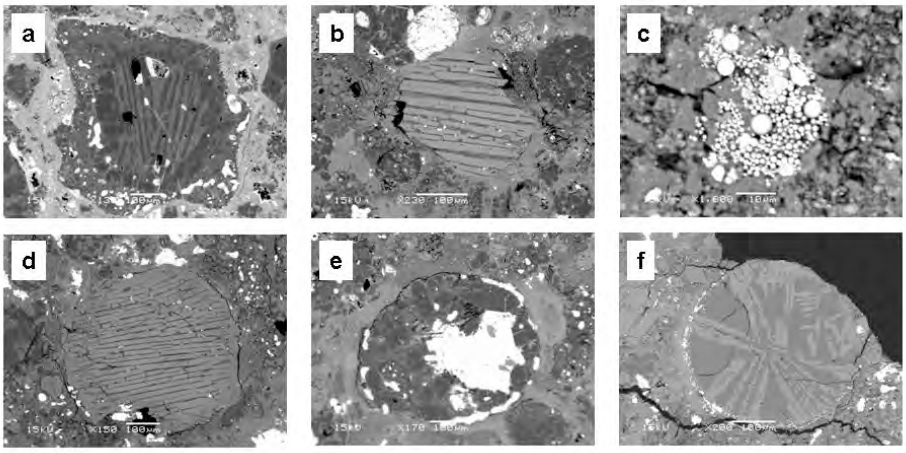

Fig 2: A collection of various back-scattered electron images showing examples of the different features

found in meteorites. Figures 2a,b,d,e, and f show a chondrule surrounded by fine-grained matrix. Figure 2a shows barred olivine within a chondrule encapsulated within another chondrule in QUE97416, Figure 2b shows barred olivine within a chondrule in Lancé, Figure 2c shows magnetite in Tagish Lake, Figure 2d shows barred olivine within a chondrule in MET00711,5 Figure 2e shows a metal grain within a chondrule in Lancé and finally, Figure 2f shows a interesting barred olivine within a chondrule within ALH83108.

The Achondrites have undergone a melting event, destroying all information about their original formation, including any pre-existing chondrules. The Chondrites still retain their nebular objects (*e.g.* chondrules, CAIs, matrix) and therefore much of the information about their formation.[1] Because the chondrites are the most common type of meteorite, the study of these make statistical conclusions useful and relevant.

Chondrites can be further divided based on their Ca/Si and Al/Si ratios and amount of matrix. Both calcium and aluminum have high condensation temperatures and are therefore the first to condense into solid material. These groups of chondrites are the enstatite chondrites, ordinary chondrites and carbonaceous chondrites. [1] This work focuses on the carbonaceous chondrites, which have the highest Ca/Si ratio (>6 at%) and Al/Si ratio (>8 at%) of the chondrites, in addition to the highest amount of matrix by volume well (>30 vol%). [2 3] Their matrix also contains carbon in the form of carbonate and/or organic compounds, as well as the presence of water in hydrous minerals making them interesting to study when considering them as a vehicle for facilitating life on Earth.

The carbonaceous chondrites do show a spectrum of alteration levels and are therefore classified with a number between 1 and 7 to reflect this alteration. The meteorites that are minimally altered are assigned the number 3 and are classified primarily by the opacity of the matrix, definition of the chondrules, and levels of mean compositional deviations of pyroxene and olivine. A type of 1-2 indicate contact with water (a 1 being more aqueous altered than a 2) and are classified by a decrease in the deviation of mean composition in pyroxene and olivine, an increase in the fine-grained nature of the matrix, and increase in the bulk carbon content. Types from 4-7 indicate heating events which are characterized by the recrystalization of the matrix, the blurring of the chondrule edges and the mean deviation of compositional variation in olivine and pyroxene decreasing to zero. [2 3]

The carbonaceous chondrites can be further divided into 7 categories (CI, CM, CB, CR, CO, CV, CK and CH)[4] based on their bulk compositions, oxygen isotopes, chondrule abundances and refractory element abundances[1]. The CO chondrites studied in this work are all type 3 and therefore are often referred to as CO3s. The CO3 chondrites show a range in amount of hydrothermal alteration and have been assigned subtypes on the basis of this level of alteration in each meteorite.

Originally, CO3 chondrites were broken into three groups, I, II and III, on the basis of the Fe content of olivine and pyroxene grains[5], then thermoluminescence was used to correlate the alteration levels with those seen in the ordinary chondrites[6]. The subtypes range from 3.0-3.8 depending on the level of alteration, 3.0 being the least altered and 3.8 being the most altered. Later, the progressive Fe enrichment of olivine in chondrules was shown to be less sensitive to terrestrial alteration[7]. The current standard is the measurement of Fe enrichment of olivine in amoeboid olivine aggregates (also known as amoeboid olivine inclusions), which are composed of smaller crystals[8]. The classification of the seven CO3 chondrites (ALH83108, A-882094, MET00694, MET00711, MET00737, QUE97416, Y-82094) into their petrologic subtypes is the main goal of this

project.

Amoeboid Olivine Aggregates (AOAs)

To determine the subtypes of these meteorites in this work, we use Amoeboid Olivine Aggregates (AOAs) as a basis of hydrothermal alteration. These are identified based on their irregular shape and composition of mostly olivine, some Anorthite ($CaAl_2Si_2O_8$) and Diopside ($CaMgSi_2O_6$), as well as the occasional presence of spinel ($MgAl_2O_4$). These objects are particularly useful to consider when classifying alteration because they are composed of small grains (5-10μm) and thus the high surface area to volume ratio of the olivine crystals make them extremely sensitive to hydrothermal alteration. As water percolates through the meteorites, Fe is dissolved into the fluid, most likely from the FeNi metal grains, Fe-rich olivine grains and Fe-bearing amorphous materials in the fine-grained matrix. Water moves along the olivine crystal boundaries and cracks, depositing a new layer of Fe-rich olivine. This creates a turtle shell-like pattern of Mg-rich olivine surrounded by ferroan olivine veins. With continued contact with water, the veins thicken and the temperature begins to rise. Eventually diffusion begins an important process creating diffusive halos, continuing the replacement of Mg-rich olivine with Fe-rich olivine. At the final subtype, 3.8, all of the Mg-rich olivine has been consumed and the Fe content of the olivine is similar to that of the surrounding matrix, indicating equilibration.

By analyzing the composition of olivine in these AOAs and calculating the ratio of forsterite to fayalite, as well as examining the thicknesses of the ferroan veins and diffusive haloes, it becomes possible to classify the petrologic subtype of each meteorite by using the methods outlined by Chizmadia et al. (2002). (Figure 3 and 4)

TABLE 4. The AOI characterstics used to refine the CO3 petrographic subtypes.

Petrographic subtype	Thicknesses of ferroan olivine veins (μm)	Thicknesses of diffusive haloes (μm)
3.0	n/a	n/a
3.1	<2	n/a
3.2	~2.5	n/a
3.3	~4	~0.5
3.4	~6	~0.6
3.5	10–15	~0.8
3.6	20–30	2–3
3.7	n/a	5–8
3.8	n/a	n/a

Abbreviations: n/a = not applicable.

Fig 3: A table from Chizmadia et. al. (2002) showing the quantification of the changes in vein size and diffusive halo size with increasing alteration. With more alteration, more Mg is replaced with Fe, increasing the size of veins and diffusive halos.

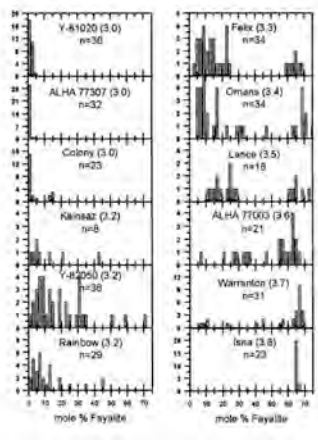

Fig 4: Histograms from Chizmadia et. al. (2002) showing the changes in the ratio of Mg-rich olivine to Fe-rich olivine as a function of analysis on the electron microprobe. An unaltered meteorite (3.0) contains olivine completely in the Mg form, whereas a completely altered meteorite (3.8) contains only Fe olivine. The stages in between illustrate the replacement of forsterite with fayalite.

Although the focus of this work is on the olivine present in these features, the secondary minerals (anorthite, diopside and spinel) are also interesting to examine, particularly through the use of x-ray element mapping to consider the affect of alteration on other elements.

Analytic Methods

Nine carbon-coated, polished meteorite thin sections were selected for analysis: ALH83108, A-882094, Lancé, MET00694:5, MET00711:5, MET00737:11, QUE97416:7, Y-82050 and Y-82094. In order to accurately analyze these features, maps were made of each thin section using the JEOL JSM5900 LV scanning electron microscope (SEM) at the Hawaii Institute for Geophysics and Planetology (HIGP) at the University of Hawaii (UH). These maps were created by assembling many individual back-scattered electron (BSE) images of the meteorite taken at a magnification of 65x, a voltage of 15kV and with a beam spot size of 56. Back-scattered electrons are those that come from the collimated beam of electrons and bounce off the sample and are collected by a detector. The number of counts is directly proportional to the atomic number of the object in the sample so therefore the whitest spots on the image are the heaviest elements. These individual images were then assembled using Photoshop to create the map. (Figure 5)

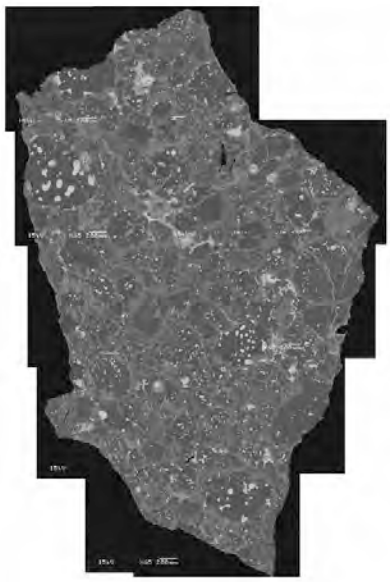

Fig 5: An example of an assembled meteorite map. This is the meteorite Y82094 thin section BSE map. This type of mapping was accomplished for all meteorites in the study.

Once maps were made, five AOAs in each meteorite were selected and imaged using the SEM to prepare for analysis on the microprobe. When relevant, interesting features in the AOAs were selected for element mapping.

Element mapping was done for 15 elements (C, O, Na, Mg, Al, Si, P, S, K, Ca, Ti, Cr, Mn, Fe, Ni). These maps are comprised of x-ray detections. These x-rays are emitted when the electron beam interacts with the sample, knocks an electron out of its shell, and the transition that occurs emits a photon whose energy corresponds to a specific atomic transition (for this analysis, these transitions are the K series). The detector collects the photons from each transition for the selected elements and a map of the locations of each element is made.

Finally, an electron microprobe (EMP) was used gather quantitative compositional data of the olivine inside the AOAs. These analyses were done using Cameca SX50 EMP for 14 elements (Si, Mg, Fe, Mn, Al, Ca, Ti, Cr, S, Na, K, P, Ni, O) using 4 crystal spectrometers, natural mineral and synthetic standards, counting times, PAP corrections, a beam current of 30nA and an acceleration voltage of 30kV. The EMP also detects the x-rays emitted from the interaction between the beam and the sample but in this case the crystal spectrometers are diffracting very specific wavelengths of energy that correspond to various atomic transitions and the detectors keep count of each detection. Three AOAs per meteorite were selected for analysis. When applicable, both Mg and Fe rich areas were analyzed. However, the BSE feature of the probe was down during the analysis so spots were found using the optical and transmitted microscope features and therefore finding the location of these features were difficult and the risk of overlapping with one of the other phases (ex: Anorthite or Diopside) when taking data was increased. In addition, the probe was down for some of the scheduled analysis periods and therefore not all meteorites were able to be analyzed.

Analysis

Microprobe data was sorted using Excel. From the EMP, we sorted the data into 3 different tables, element%, atomic% and oxide%. First, each table was sorted according to total. Only totals between 97-100 % were acceptable for analysis. Next, Ca, Al and S values were considered for each table. For element% and Atomic%, amounts greater than .1, .1 and .8 for Al Ca and S were eliminated, respectively. For Oxide%, values greater than 1, 1 and .1 for Ca, Al and S were eliminated, respectively. Finally the stoichiometry of the minerals was considered. If the Al and Ca had a 2/1+/-0.1 ratio in the Element % table and the Al, Ca and S values were reasonable but perhaps slightly out of range, indicating that our beam had overlapped with Anorthite. We left these analyses in the data, as it does not affect the resultant Fe/Mg ratio. Next we went through each table keeping in mind that each table reflected a different sensitivity based on the atomic number so we only eliminated a data point if it was truly out of range in all tables. Finally, the remaining data points were sorted, and the forsterite to fayalite ratios were calculated by dividing the at% Fe by the sum of at% Fe and at% Mg. From this, histograms were made detailing the distributions of these ratios as a function of the number of analyses so that conclusions could be made.

Results and Discussion

Our analysis of the previously studied meteorites Lancé and Y82050 showed an agreement with the previous studies, although an offset is present in the histogram peaks between our data and that from previous studies and is being further investigated.

Using the distribution of Fe in the olivine (Figures 6 and 7) we have assigned petrologic subtypes to the five CO3 chondrites: ALH83108, MET00694, MET00711, MET00737, QUE97416 (Table 1).

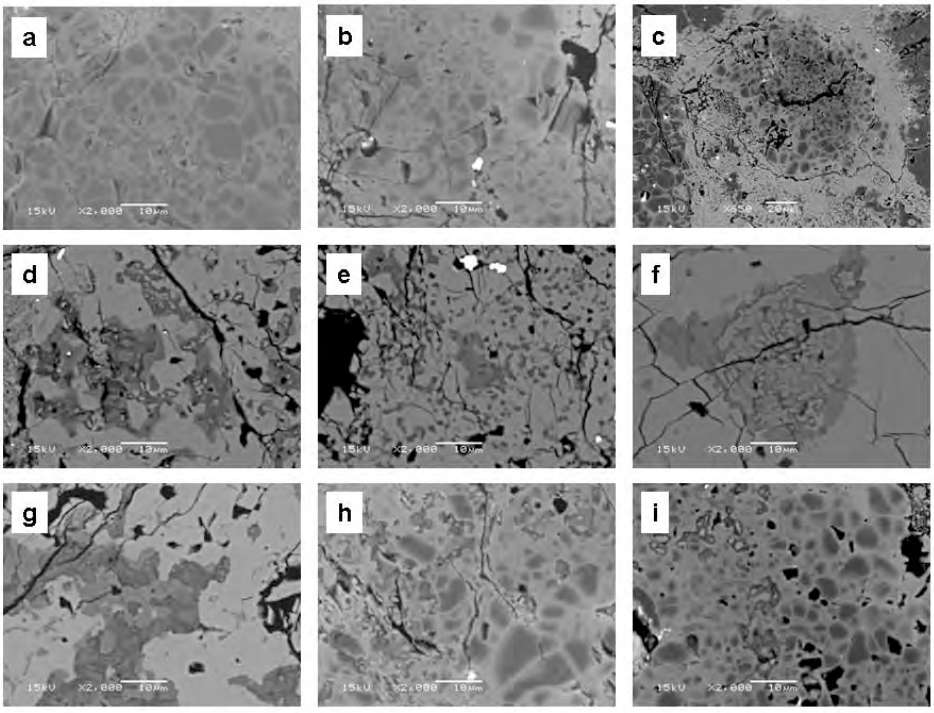

Figure 6: Showing the high resolution (2,000x, with the exception of Fig 6c, which is at 450x) BSE images taken of representative AOAs in each meteorite. Figure 6a: Y82050, 6b: Lancé 6c: Y82094, 6d: MET00694, 6e: MET00711, 6f: MET00737, 6g: ALH83108, 6h: QUE97416, 6i: A882094.

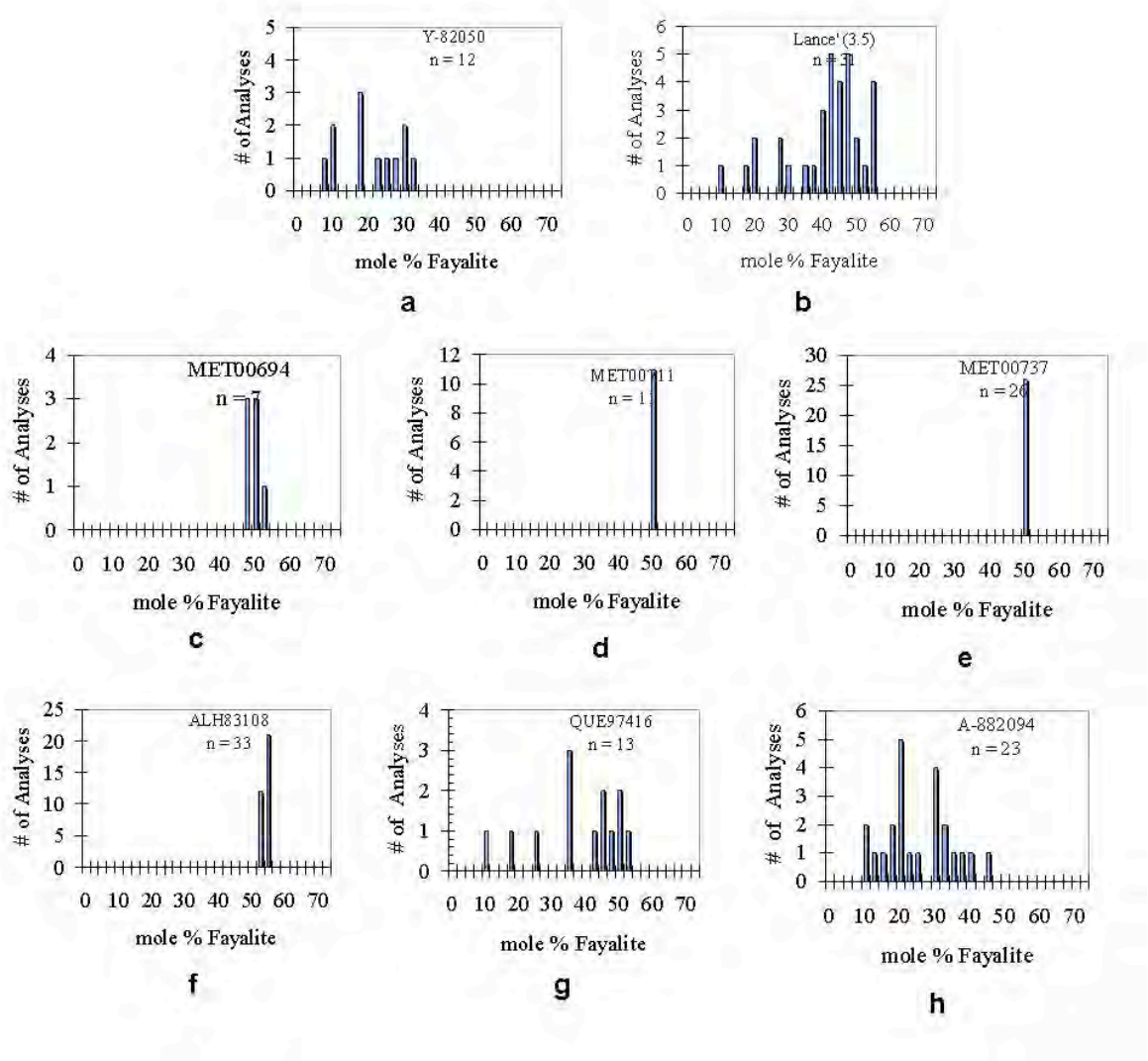

Figure 7: Showing the resultant histograms of the EMP analysis of each meteorite. Figure 7a: Y82050, 7b: Lancé 7c: Y82094, 7d: MET00694, 7e: MET00711, 7f: MET00737, 7g: ALH83108, 7h: QUE97416, 7i: A882094.

Meteorite	Petrologic Subtype
Y-82050	3.2
Y-82094	3.3
A882094	3.4
Lancé	3.5
QUE97416	3.5
ALH83108	3.8

MET00694	3.8
MET00711	3.8
MET00737	3.8

Table 1: Showing the results of subtype classification for the meteorites in our study.

We classified QUE97416 to be a 3.5, ALH83108 to be a 3.8, and the three MET chondrites to be 3.8 The MET meteorites were hypothesized to be paired based on the location in which they were found, and their identical assigned subtypes suggest that this is indeed the case. The five AOAs identified in A-882094 each show a different level of alteration and therefore we suspect this meteorite of being the first CO3 breccia to be reported. We were unable to analyze the olivine in Y-82094 due to difficulties with the probe, but we have estimated its subtype to be 3.3 by comparing the AOAs to those from Chizmadia *et al.* 2002 (Figure 8).

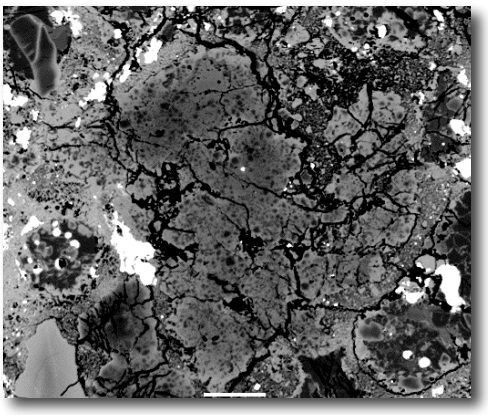

Figure 8: ALH82101, a 3.3 meteorite analyzed by Chizmadia et al. in 2002, on which we base our 3.3 classification of Y-82094.

Results and Discussion: Element Maps

Although the primary focus of this paper is to assign subtypes to CO3 chondrites which have previously not been investigated in detail, an examination of how other elements are moving based on subtype was a secondary goal. We focused specifically on the four phases (Olivine, Anorthite, Diopside, and sometimes Spinel) present in the more altered meteorites, along with the turtle shell pattern found in the less altered meteorites. Figures 9-15 show representative examples of 6 element maps. These element maps reinforced our identification of the various minerals present in the meteorites, as well as illustrating how the AOAs are equilibrating with the matrix (e.g. Mg “hot” spots and Fe “cold” spots vs. a fairly even distribution of Mg and Fe). In addition, these maps suggest in some cases that Na is moving into the Anorthite and replacing it, most likely by nepheline or sodalite.

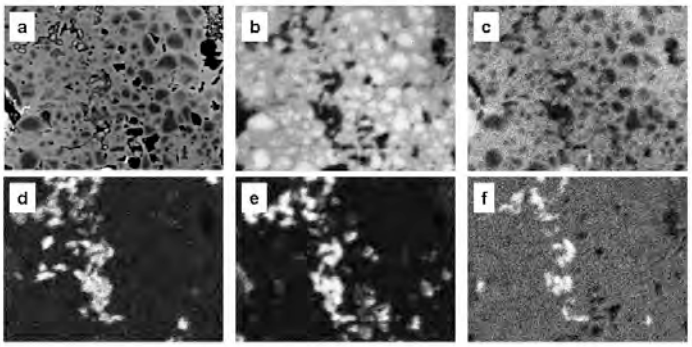

Figure 9: The element maps of A882094 AOA#3. a: BSE image, b: Mg map, c: Fe map, d: Ca map, e: Al map, f: Na map. The AOA has not yet equilibrated with the matrix as evidenced by the Mg hot spots in 9b. reinforcing the classification of a lesser altered meteorite. In addition, 9f demonstrates the attack of Na on the Anorthite.

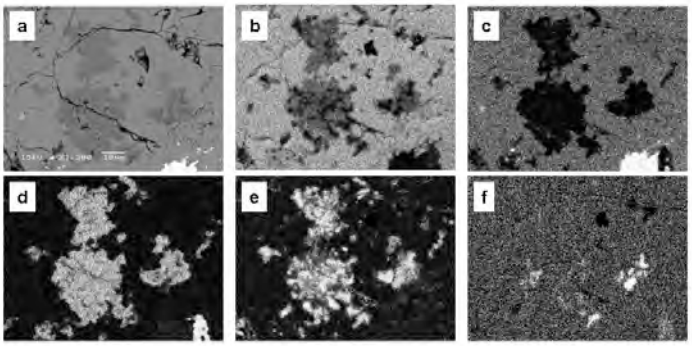

Figure 10: The element maps of MET00694 AOA#4. a: BSE image, b: Mg map, c: Fe map, d: Ca map, e: Al map, f: Na map. In this figure the Anorthite and Diopside dominate, and a well equilibrated matrix is obvious indicating a well altered meteorite.

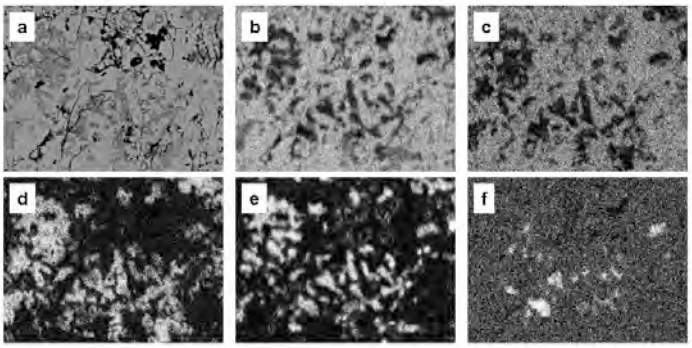

Figure 11: The element maps of MET00711 AOA#5. a: BSE image, b: Mg map, c: Fe map, d: Ca map, e: Al map, f: Na map. In this figure the Anorthite and Diopside dominate, and some spinel regions can be seen, and a well equilibrated matrix is again obvious.

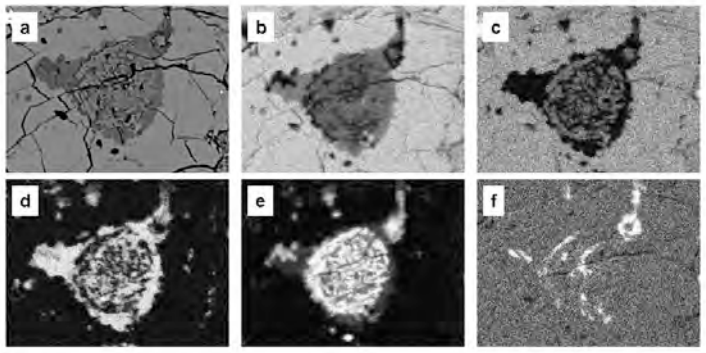

Figure 12: The element maps of MET00737 AOA#1. a: BSE image, b: Mg map, c: Fe map, d: Ca map, e: Al map, f: Na map. In this figure the Anorthite and Diopside dominate, and some spinel regions can be seen, and a well equilibrated matrix is again obvious.

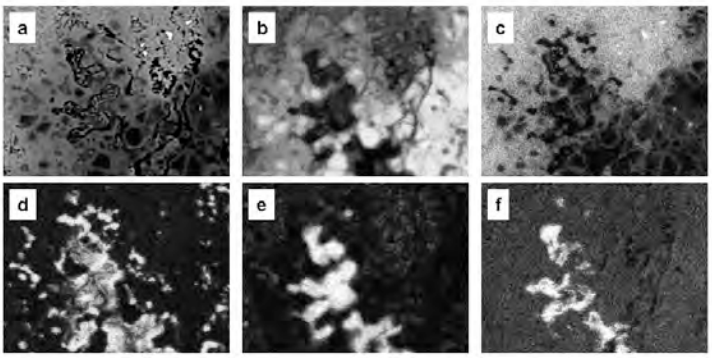

Figure 13: The element maps of QUE94716 AOA#2. a: BSE image, b: Mg map, c: Fe map, d: Ca map, e: Al map, f: Na map. In this figure both the turtle shell pattern and Anorthite and Diopside regions can be seen, in addition to the attack of Anorthite by Na.

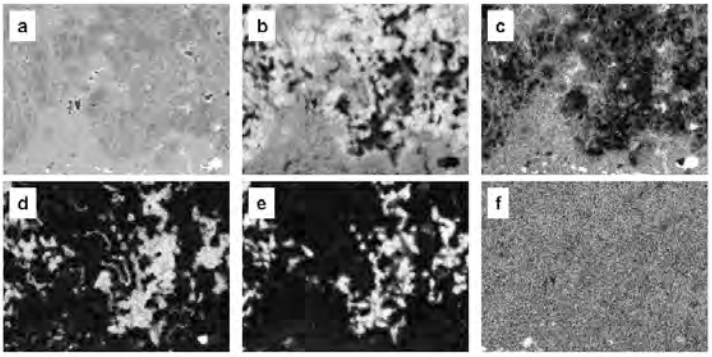

Figure 14: The element maps of Y82040 AOA#2. a: BSE image, b: Mg map, c: Fe map, d: Ca map, e: Al map, f: Na map. In this figure both the turtle shell pattern with Mg hot spots and Anorthite and Diopside regions can be seen.

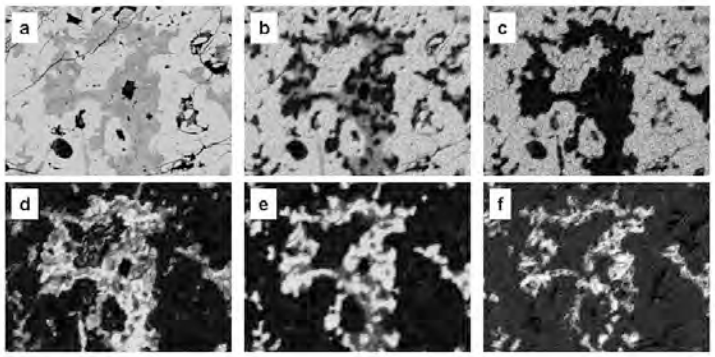

Figure 15: The element maps of ALH83108 AOA#5. a: BSE image, b: Mg map, c: Fe map, d: Ca map, e: Al map, f: Na map. A well-equilibrated AOA, as well as a good example of the Na attack on Anorthite.

Conclusions

Based on our results, we can augment the pre-existing body of subtype classification of CO3 chondrites. Because it is hypothesized that every CO3 meteorite that falls is part of the same parent body, statistical conclusions drawn about the distribution of subtypes of this type of meteorite based on the weight of the recovered fragment will lend it self to the development of a parent body alteration model. (Figure 16)

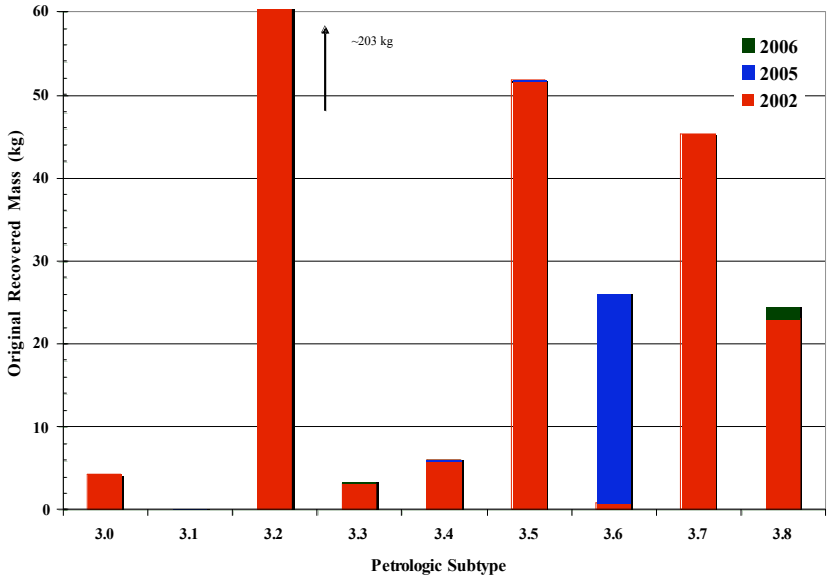

Figure 16: The distribution of classified meteorites by weight (kg) vs. petrologic subtype.

This will give us better understanding about the distribution of heat and water on an asteroid, as well as giving insight into the conditions of heat and water in the early solar system as well.

Future work

As this is part of a larger project, there is still much to be contributed. Specifically relevant to this work, more AOAs from meteorites presented will be analyzed to augment the statistics of the EMP data. In addition, more CO3 meteorites will be requested and

analyzed. Further element maps will be taken to gain more understanding into how secondary elements are moving as a function of alteration (*e.g.* does Na replacement of anorthite increase with higher subtypes?). Finally, an emphasis on studying the 3.1 meteorites will help us better understand the initial stages of alteration, the mechanisms involved in the replacement of olivine and how it compares to the aqueous alteration of other groups of chondrites (*e.g.* ordinary chondrites and other carbonaceous chondrite groups).

Acknowledgements

Lysa Chizmadia for being a fantastic and patience mentor and a wonderful resource, Jonathan Williams for heading up a great REU program, the other REU students for their support, discussion, and entertainment, NSF for funding the REU program, the faculty and grad students at the IfA for sharing their research and free time, Gary Huss for SEM assistance, and finally Sarah Sherman for EMP assistance. Thanks for a great summer!

References

[1] McSween, Jr. H.Y. Meteorites and Their Parent Planets. Cambridge University Press, Cambridge, UK: 1987.

[2] Wasson, J.T. Meteorites: Their Record of Early Solar-System History. W.H. Freeman and Col, USA: 1985

[3] Sears, D.W.G. and Dodd, R.T.. "Overview and Classification of Meteorites" from Meteorites and the Early Solar System. University of Arizona Press, USA: 1988.

[4] McSween, Jr. H. Y., Sears, D.W.G, Dodd, R. T. "Thermal Metamorphism" from Meteorites and the Early Solar System. University of Arizona Press, USA: 1988.

[5] McSween, Jr. H.Y. "Carbonaceous chondrites of the Ornans type: a metamorphic sequence" Geochimica et Cosmochimica Acta. 1977 Col 41 pp 477-491.

[6] Keck, Bradly D., Sears, Derek W. G. "Chemical and physical studides of type 3 chondrites—VII: Thermoluminescence and metamorphism in the CO chondrites" Geochimica et Cosmochimica Acta 1987 Vol. 51, pp. 3013-3021.

[7] Scott, Edward R.D., Jones, Rhian H. "Disentabngling nebular and asteroidal features of CO3 carbonaceous chondrite meteorites". Geochimica et. Cosmochimica Acta. 1990 Vol. 54, pp 2485-2502.

[8] Chizmadia, Lysa J., Rubin, Alan El, Wasson, John T. "Mineralogy and petrology of amoeboid olivine inclusions in CO3 chondrites: Relationship to parent-body aqueous alteration." Meteroties & Planetary Science 2002 Vol. 31, pp 1781-1796.